

Applications of Mathematics

Dominique Jeulin

Iterated Boolean random varieties and application to fracture statistics models

Applications of Mathematics, Vol. 61 (2016), No. 4, 363–386

Persistent URL: <http://dml.cz/dmlcz/145791>

Terms of use:

© Institute of Mathematics AS CR, 2016

Institute of Mathematics of the Czech Academy of Sciences provides access to digitized documents strictly for personal use. Each copy of any part of this document must contain these *Terms of use*.



This document has been digitized, optimized for electronic delivery and stamped with digital signature within the project *DML-CZ: The Czech Digital Mathematics Library* <http://dml.cz>

ITERATED BOOLEAN RANDOM VARIETIES AND APPLICATION
TO FRACTURE STATISTICS MODELS

DOMINIQUE JEULIN, Fontainebleau

(Received March 15, 2016)

Abstract. Models of random sets and of point processes are introduced to simulate some specific clustering of points, namely on random lines in \mathbb{R}^2 and \mathbb{R}^3 and on random planes in \mathbb{R}^3 . The corresponding point processes are special cases of Cox processes. The generating distribution function of the probability distribution of the number of points in a convex set K and the Choquet capacity $T(K)$ are given. A possible application is to model point defects in materials with some degree of alignment. Theoretical results on the probability of fracture of convex specimens in the framework of the weakest link assumption are derived, and used to compare geometrical effects on the sensitivity of materials to fracture.

Keywords: Boolean model; Boolean varieties; Cox process; weakest link model; fracture statistics; mathematical morphology

MSC 2010: 60G55, 60D05, 52A22

1. INTRODUCTION

Point processes showing clustering effects are interesting models to simulate non-homogeneous location of points in space, as seen for instance for some defects in materials: for polycrystals modelled by random tessellations, defects can be located on the grain boundaries; in composite materials, they can appear on fibers of a network. The aim of this paper is to introduce some random sets models based on point processes reproducing these kinds of situation, and to study some of their theoretical probabilistic properties.

After a reminder on random sets obtained from Boolean random varieties in \mathbb{R}^n , two-steps varieties in \mathbb{R}^n are introduced and characterized. The cases of point processes in \mathbb{R}^2 and in \mathbb{R}^3 are detailed to generate random points on lines and on planes. A three-steps Poisson points process in \mathbb{R}^3 enables us to take into account alignments in Poisson planes. All these point processes are particular cases of Cox point pro-

cesses, for which the generating function of the probability distribution of the number of points in a convex set K and the Choquet capacity $T(K)$ are calculated.

In the last section, we make use of iterated Boolean varieties to propose new probabilistic models of fracture based on the weakest link assumption, which can be applied to model the intergranular fracture of polycrystals or the fiber fracture of composites.

2. REMINDER ON BOOLEAN RANDOM VARIETIES

In this section we give the construction of Boolean random sets based on random varieties in \mathbb{R}^n , and establish their main probabilistic properties, namely their Choquet capacity.

2.1. Construction and properties of the linear Poisson varieties model in \mathbb{R}^n . A geometrical introduction of the Poisson linear varieties is as follows (see [12]). Consider in \mathbb{R}^n any linear variety with dimension $n - k$ containing the origin O , and with orientation ω . A Poisson point process $\{x_i(\omega)\}$ with intensity $\theta_k(d\omega)$ is generated on the variety with orientation ω . On every point $x_i(\omega)$ a variety $V_k(\omega)_{x_i}$ with dimension k , is located orthogonal to the direction ω . By construction, we have $V_k = \bigcup_{x_i(\omega)} V_k(\omega)_{x_i}$. For instance in \mathbb{R}^3 we can build a network of Poisson hyperplanes Π_α (orthogonal to the lines D_ω containing the origin) or a network of Poisson lines in every plane Π_ω containing the origin.

Definition 1. In \mathbb{R}^n , n Poisson linear varieties V_k of dimension k ($k = 0, 1, \dots, n - 1$) can be built: the Poisson point process for $k = 0$, and the Poisson hyperplanes for $k = n - 1$. For $k \geq 1$, a network of Poisson linear varieties of dimension k can be considered as a Poisson point process in the space $S_k \times \mathbb{R}^{n-k}$, the cross product of orientations S_k of linear varieties of dimension $n - k$ and of the Euclidean space \mathbb{R}^{n-k} , with intensity $\theta_k(d\omega)\mu_{n-k}(dx)$; θ_k is a positive Radon measure for the set of subspaces S_k of dimension k , and μ_{n-k} is the Lebesgue measure of \mathbb{R}^{n-k} . For instance, Poisson lines in \mathbb{R}^2 can be considered as a Poisson point process on the space $[0, \pi] \times \mathbb{R}$.

If $\theta_k(d\omega)$ is any Radon measure, the varieties obtained are anisotropic. When $\theta_k(d\omega) = \theta_k d\omega$, the varieties are isotropic. If the Lebesgue measure $\mu_{n-k}(dx)$ is replaced by a measure $\theta_{n-k}(dx)$, non stationary random varieties are obtained.

The probabilistic properties of the Poisson varieties are easily derived from their definition as a Poisson point process.

Theorem 1. *The number of varieties of dimension k hit by a compact set K is a Poisson variable, with parameter $\theta(K)$:*

$$(2.1) \quad \theta(K) = \int \theta_k(d\omega) \int_{K(\omega)} \theta_{n-k}(dx) = \int \theta_k(d\omega) \theta_{n-k}(K(\omega)),$$

where $K(\omega)$ is the orthogonal projection of K on the orthogonal space to $V_k(\omega)$, $V_{k^\perp}(\omega)$. For the stationary case,

$$(2.2) \quad \theta(K) = \int \theta_k(d\omega) \mu_{n-k}(K(\omega)).$$

The Choquet capacity $T(K) = P\{K \cap V_k \neq \emptyset\}$ of the varieties of dimension k is given by

$$(2.3) \quad T(K) = 1 - \exp\left(- \int \theta_k(d\omega) \int_{K(\omega)} \theta_{n-k}(dx)\right).$$

In the stationary case, the Choquet capacity is

$$(2.4) \quad T(K) = 1 - \exp\left(- \int \theta_k(d\omega) \mu_{n-k}(K(\omega))\right).$$

Proof. By construction, the random varieties $V_k(\omega)$ induce by intersection on every orthogonal variety of dimension $n - k$, $V_{k^\perp}(\omega)$, a Poisson point process with dimension $n - k$ and with intensity $\theta_k(d\omega)\theta_{n-k}(dx)$. Therefore, the contribution of the direction ω to $N(K)$ is the Poisson variable $N(K, \omega)$ with intensity $\theta_{n-k}(K(\omega))$. Since the contributions of the various directions are independent, Equation (2.1) results immediately. \square

Proposition 2. *Consider now the isotropic (θ_k being constant) and stationary case, and a convex set K . Due to the symmetry of the isotropic version, we can consider $\theta_k(d\omega) = \theta_k d\omega$ as defined on the half unit sphere (in \mathbb{R}^{k+1}) of the directions of the varieties $V_k(\omega)$. The number of varieties of dimension k hit by a compact set K is a Poisson variable, with parameter $\theta(K)$ given by:*

$$(2.5) \quad \theta(K) = \theta_k \int \mu_{n-k}(K(\omega)) d\omega = \theta_k \frac{b_{n-k} b_{k+1}}{b_n} \frac{k+1}{2} W_k(K),$$

where b_k is the volume of the unit ball in \mathbb{R}^k ($b_k = \pi^{k/2}/\Gamma(1+k/2)$, $b_1 = 2$, $b_2 = \pi$, $b_3 = \frac{4}{3}\pi$), and $W_k(K)$ is Minkowski's functional of K , homogeneous and of degree $n - k$ (see [12]).

The following examples are useful for applications:

- ▷ When $k = n - 1$, the varieties are Poisson planes in \mathbb{R}^n ; in that case, $\theta(K) = \theta_{n-1}nW_{n-1}(K) = \theta_{n-1}\mathcal{A}(K)$, where $\mathcal{A}(K)$ is the norm of K (average projected length over orientations).
- ▷ In the plane \mathbb{R}^2 the Poisson lines are obtained, with $\theta(K) = \theta L(K)$, L being the perimeter.
- ▷ In the three-dimensional space \mathbb{R}^3 , Poisson lines for $k = 1$ and Poisson planes for $k = 2$ are obtained. For Poisson lines, $\theta(K) = \frac{1}{4}\pi\theta S(K)$ and for Poisson planes, $\theta(K) = \theta M(K)$, where S and M are the surface area and the integral of the mean curvature, respectively.

2.2. Boolean random varieties. Boolean random sets can be built starting from Poisson varieties and a random primary grain [4], [5], [9].

Definition 2. A Boolean model with primary grain A' is built on Poisson linear varieties in two steps: i) we start from a network V_k ; ii) every variety $V_{k\alpha}$ is dilated by an independent realization of the primary grain A' . The Boolean RACS A is given by

$$A = \bigcup_{\alpha} V_{k\alpha} \oplus A'.$$

By construction, this model induces on every variety $V_{k\perp}(\omega)$ orthogonal to $V_k(\omega)$ a standard Boolean model with dimension $n - k$, with random primary grain $A'(\omega)$ and with intensity $\theta(\omega) d\omega$. The Choquet capacity of this model immediately follows, after averaging over the directions ω ; it can also be deduced from Equation (2.4), after replacing K by $A' \oplus \check{K}$ and averaging.

Theorem 3. *The Choquet capacity of the Boolean model built on Poisson linear varieties of dimension k is given by*

$$(2.6) \quad T(K) = 1 - \exp\left(-\int \theta_k(d\omega) \bar{\mu}_{n-k}(A'(\omega) \oplus \check{K}(\omega))\right).$$

For isotropic varieties, the Choquet capacity of Boolean varieties is given by

$$(2.7) \quad T(K) = 1 - \exp\left(-\theta_k \frac{b_{n-k}b_{k+1}}{b_n} \frac{k+1}{2} \bar{W}_k(A' \oplus \check{K})\right).$$

Particular cases of Equation (2.6) are obtained when $K = \{x\}$ (giving the probability $q = P\{x \in A^c\} = \exp(-\int \theta_k(d\omega) \mu_{n-k}(A'(\omega)))$) and when $K = \{x, x + h\}$, giving the covariance of A^c , $Q(h)$:

$$(2.8) \quad Q(h) = q^2 \exp\left(\int \theta_k(d\omega) K_{n-k}(\omega, \vec{h} \cdot \vec{u}(\omega))\right)$$

where $K_{n-k}(\omega, h) = \bar{\mu}_{n-k}(A'(\omega) \cap A'_{-h}(\omega))$ and $\vec{u}(\omega)$ is the unit vector with the direction ω . For a compact primary grain A' , there exists for any h an angular sector where $K_{n-k}(\omega, h) \neq 0$, so that the covariance generally does not reach its sill, at least in the isotropic case, and the integral range, obtained by integration of the correlation function, is infinite. Consider now some examples in \mathbb{R}^2 and in \mathbb{R}^3 .

2.2.1. Fibers in 2D. In the plane a Boolean model on Poisson lines can be built. For an isotropic lines network (Figure 1), and if $A' \oplus \check{K}$ is a convex set, we have, from equation (2.7):

$$(2.9) \quad T(K) = 1 - \exp(-\theta \bar{L}(A' \oplus \check{K})).$$

If $A' \oplus \check{K}$ is not a convex set, the integral of projected lengths over a line with the orientation varying between 0 and π must be taken. If A' and K are convex sets, we have $\bar{L}(A' \oplus \check{K}) = \bar{L}(A') + L(K)$. Consider now the isotropic case. Using for A' a random disc with a random radius R (with expectation \bar{R}) and for K a disc with radius r , equation (2.9) becomes

$$\begin{aligned} T(r) &= 1 - \exp(-2\pi\theta(\bar{R} + r)), \\ T(0) &= P\{x \in A\} = 1 - \exp(-2\pi\theta\bar{R}), \end{aligned}$$

which can be used to estimate θ and \bar{R} , and to validate the model.

In \mathbb{R}^3 , a Boolean model on Poisson planes or on Poisson lines can be built.

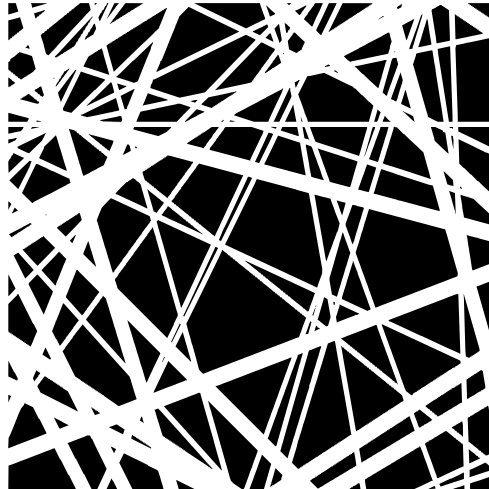


Figure 1. Example of Boolean model built on Poisson lines (1024 × 1024 image), using as primary grains discs with radius 5 (with probability 0.75) and 15 (with probability 0.25).

2.2.2. Boolean model on Poisson planes in \mathbb{R}^3 . A Boolean model built on Poisson planes generates a structure with strata. On isotropic Poisson planes, we have for a convex set $A' \oplus \check{K}$ by application of equation (2.7):

$$(2.10) \quad T(K) = 1 - \exp(-\theta \overline{M}(A' \oplus \check{K})).$$

When A' and K are convex sets, we have $\overline{M}(A' \oplus \check{K}) = \overline{M}(A') + M(K)$. If $A' \oplus \check{K}$ is not convex, $T(K)$ is expressed as a function of the length l of the projection over the lines D_ω by $T(K) = 1 - \exp(-\theta \int_{2\pi \text{ ster}} \overline{l}(A'(\omega) \oplus \check{K}(\omega)) d\omega)$. For instance if A' is a random sphere with a random radius R (with expectation \overline{R}) and K is a sphere with radius r , equation (2.10) becomes:

$$\begin{aligned} T(r) &= 1 - \exp(-4\pi\theta(\overline{R} + r)), \\ T(0) &= P\{x \in A\} = 1 - \exp(-4\pi\theta\overline{R}), \end{aligned}$$

which can be used to estimate θ and \overline{R} , and to validate the model.

2.2.3. Boolean model on Poisson lines in \mathbb{R}^3 . A Boolean model built on Poisson lines generates a fiber network, with possible overlaps of fibers, as illustrated in Figure 2. On isotropic Poisson lines, we have for a convex set $A' \oplus \check{K}$

$$(2.11) \quad T(K) = 1 - \exp\left(-\theta \frac{\pi}{4} \overline{S}(A' \oplus \check{K})\right).$$

If $A' \oplus \check{K}$ is not a convex set, $T(K)$ is expressed as a function of the area A of the projection over the planes Π_ω by

$$(2.12) \quad T(K) = 1 - \exp\left(-\frac{1}{2}\theta \int_{2\pi \text{ ster}} \overline{A}(A'(\omega) \oplus \check{K}(\omega)) d\omega\right).$$

If A' is a random sphere with a random radius R (with expectation \overline{R} and second moment $E(R^2)$) and K is a sphere with radius r , equation (2.11) becomes

$$\begin{aligned} T(r) &= 1 - \exp(-\pi^2\theta(E(R^2) + 2r\overline{R} + r^2)), \\ T(0) &= P\{x \in A\} = 1 - \exp(-\pi^2\theta E(R^2)), \end{aligned}$$

which can be used to estimate θ , $E(R^2)$ and \overline{R} , and to validate the model. A model of Poisson fibers parallel to a plane, and with a uniform distribution of orientations in the plane, was used to model cellulosic fiber materials (see [1]). In [14], non isotropic dilated Poisson lines were used to model and to optimize the acoustic absorption of nonwoven materials. In [2], elastic properties of isotropic fiber networks were studied by numerical simulations.

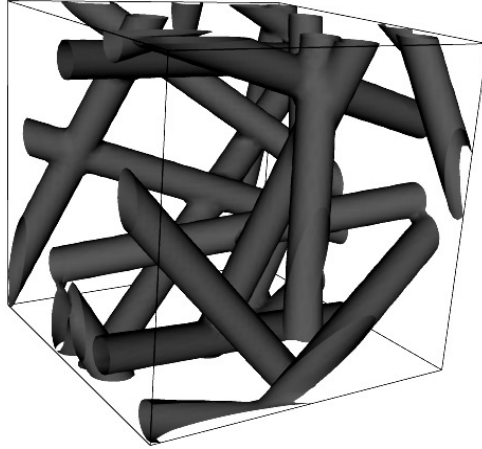


Figure 2. Simulation of Poisson fibers with a single radius in 3D (see [3]).

3. TWO STEPS BOOLEAN VARIETIES

It is possible to generate further Boolean models by iteration of Poisson varieties. For instance in \mathbb{R}^2 , we first consider Poisson lines, and in the second step Poisson points on every line. These points are germs to locate primary grains A' to generate a Boolean model. Compared to the standard Boolean model, this one shows alignments of grains. Similarly in \mathbb{R}^3 we can start from Poisson planes $V_{2\alpha}$ and use Poisson lines $V_{1\beta}$ in every plane to generate a Boolean model with fibers. In contrast to Poisson fibers in \mathbb{R}^3 , this model generates a random set with some coplanar fibers. Such long range random sets could mimic specific microstructures with an order in a lower dimension subspace of \mathbb{R}^n , such as preferred germination of objects on specific planes or lines.

These models are based on doubly stochastic Poisson random variables for which the Choquet capacity can be obtained. In other contexts, iterations of random tessellations were proposed as models of a random set, like the STIT tessellations related to the fracture process of materials (see [13]), or iterated division of cells to simulate telecommunication networks (see [11]).

Definition 3. Two steps random varieties are defined as follows: starting from Poisson linear varieties V_k of dimension k and with intensity $\theta_k(d\omega)$ in \mathbb{R}^n , Poisson linear varieties $V_{k'\beta}$ with dimension $0 \leq k' < k$ and with intensity $\theta_{k'}(d\omega)$ are located on each $V_{k\alpha}$. Then each $V_{k'\beta}$ is dilated by independent realizations of a random compact primary grain $A' \subset \mathbb{R}^n$ to generate the Boolean RACS A :

$$A = \bigcup_{\beta} V_{k'\beta} \oplus A'.$$

Remark 1. By construction, when $k' = 0$ the varieties $V_{k'\beta}$ are a particular case of a Cox process driven by the random set V_k , and the derived random set A is a Cox Boolean model (see [8]).

In what follows the purpose is restricted to the stationary and isotropic case, with two intensities θ_k and $\theta_{k'}$.

Theorem 4. *The number $N(K)$ of varieties of dimension $k' < k$ hit by the compact set K is a random variable with the generating function*

$$(3.1) \quad G_{k'}(s, K) = E\{s^{N(K)}\} = \exp[\theta_k a_k W_k(K)[\varphi_{k'}(\theta_{k'} a_{k'}(1-s), K) - 1]],$$

where $a_{k'} = \frac{1}{2}(k' + 1)b_{n-k'}b_{k'+1}/b_n$ and $\varphi_{k'}(\lambda, K)$ is the Laplace transform of the random variable $W_{k'}(K \cap V_{k\alpha})$, $W_{k'}$ being the Minkowski functional homogeneous with degree $k - k'$ in \mathbb{R}^k :

$$(3.2) \quad \varphi_{k'}(\lambda, K) = E\{\exp[-\lambda W_{k'}(K \cap V_k)]\},$$

the mathematical expectation being taken over the realizations $V_{k\alpha}$. As a consequence, the Choquet capacity of the Boolean RACS A built on the Poisson linear varieties $V_{k'}$ using a deterministic primary grain A' is derived from $G_{k'}(0, A' \oplus \check{K})$, $E\{\}$ being the expectation with respect to the random variety $V_{k\alpha}$:

$$(3.3) \quad 1 - T(K) = \exp[-\theta_k a_k W_k(A' \oplus \check{K})[1 - E\{\exp[-\theta_{k'} a_{k'} W_{k'}(A' \oplus \check{K} \cap V_k)]\}]].$$

Proof. The random number N_k of varieties $V_{k\alpha}$ hit by K is a Poisson variable with expectation $\theta_k a_k W_k(K)$. On each $V_{k\alpha}$, $N_{k'}$ varieties $V_{k'\beta}$ are generated, $N_{k'}$ being a Poisson variable with expectation $\theta_{k'} a_{k'} W_{k'}(K \cap V_k)$. For a random section $K \cap V_{k\alpha}$, the generating function of $N_{k'}$ is

$$(3.4) \quad \Gamma(s) = \exp[-\theta_{k'} a_{k'} W_{k'}(K \cap V_{k\alpha})(1-s)].$$

Taking the expectation of (3.4) with respect to $W_{k'}(K \cap V_{k\alpha})$ and then of $\Gamma(s)^{N_k}$ gives (3.1). □

The Choquet capacity requires the use of the Laplace transform $\varphi_{k'}(\lambda, A' \oplus \check{K})$. It is not easy to express them in a closed form for specific compact sets K and A' . However, the required distribution functions and their Laplace transforms can be estimated by simulation of the random variables obtained from random variables $W_{k'}(A' \oplus \check{K} \cap V_{k\alpha})$ obtained from random sections. Examples of closed form expressions are given now for two-steps Poisson points in \mathbb{R}^2 and in \mathbb{R}^3 .

3.1. Poisson points on Poisson lines in the plane. Starting from Poisson lines in the plane, a 1D Poisson point process is independently generated on each line.

Proposition 5. *The generating function $G_K(s)$ of the random number of points $N_P(K)$ contained in a convex set K in \mathbb{R}^2 with perimeter $\mathcal{L}(K)$, random intercept length $L(K)$ (with Laplace transform $\varphi_L(\lambda, K)$), is given by*

$$(3.5) \quad G_K(s) = \exp(-\theta_1 \mathcal{L}(K)(1 - \varphi_L(\theta(1 - s), K))).$$

We have

$$(3.6) \quad 1 - T(K) = Q(K) = \exp(-\theta_1 \mathcal{L}(K)(1 - \varphi_L(\theta, K))).$$

The Choquet capacity of the corresponding Boolean model for convex sets K and A' is obtained by replacing K by $(A' \oplus \check{K})$ in equation (3.6).

Proof. The set K hits a Poisson random number of lines N_D with parameter $\theta_1 \mathcal{L}(K)$. Each chord with random length $L(K)$ contains a Poisson number of points with parameter $\theta L(K)$ and generating function

$$\Gamma(s, L(K)) = \exp(-\theta L(K)(1 - s)).$$

After deconditioning with respect to $L(K)$, with Laplace transform $\varphi_L(\lambda, K)$, we obtain the generating function $\Gamma(s, K) = E_L\{\Gamma(s, L(K))\} = \varphi_L(\theta(1 - s), K)$. Then we consider the sum of N_D realizations of the random variable $L(K)$ to obtain equation (3.5) by expectation with respect to N_D :

$$G_K(s) = E_{N_D}\{\varphi_L(\theta(1 - s), K)^{N_D}\} = \exp(\theta_1 \mathcal{L}(K)(\varphi_L(\theta(1 - s), K) - 1)).$$

□

When K is the disc $C(r)$ with radius r , the generating function of the random number of points $N_P(r)$ in $C(r)$ is obtained by

$$G(s, r) = \exp[-2\pi r \theta_1(1 - \varphi_L(\theta(1 - s), r))]$$

with $\varphi_L(\lambda, r)$ given by equation (7.1) or 7.2. We have

$$Q(r) = \exp[-2\pi r \theta_1(1 - \varphi_L(\theta, r))].$$

3.2. Poisson points on Poisson planes in \mathbb{R}^3 . This point process is obtained in two steps:

- (1) We start with Poisson planes in \mathbb{R}^3 (consider here the isotropic case), with intensity θ_2 .
- (2) On each Poisson plane, a 2D Poisson point process is generated, with intensity θ .

Proposition 6. *The generating function $G_K(s)$ of the random number of points $N_P(K)$ contained in a convex set K is given by*

$$(3.7) \quad G_K(s) = \exp[-\theta_2 M(K)(1 - \psi_A(\theta(1 - s), K \cap \pi))]$$

and we get

$$(3.8) \quad 1 - T(K) = Q(K) = \exp[-\theta_2 M(K)(1 - \psi_A(\theta, K \cap \pi))]$$

with $M(K)$: integral of mean curvature of K ; $A(K \cap \pi)$: area of sections of K by a random plane π , with Laplace transform $\psi_A(\lambda, K \cap \pi)$.

The Choquet capacity of the corresponding Boolean model for convex sets K and A' is obtained by replacing K by $(A' \oplus \check{K})$ in equation (3.8).

P r o o f. The random number of planes $N_\pi(K)$ hit by K is a Poisson variable with parameter $\theta_2 M(K)$. Each plane π cuts K along a convex random set with area $A(K \cap \pi)$, containing a Poisson number of points, with parameter $\theta A(K)$ and generating function

$$\Gamma(s, A(K)) = \exp(-\theta A(K)(1 - s)).$$

After deconditioning with respect to $A(K)$, with Laplace transform $\psi_A(\lambda, K \cap \pi)$, we obtain the generating function $\Gamma(s, K) = E_A\{\Gamma(s, A(K))\} = \psi_A(\theta(1 - s), K \cap \pi)$. Then we consider the sum of N_π realizations of the random variable $A(K)$ to obtain equation (3.7) by expectation with respect to N_π :

$$\begin{aligned} G_K(s) &= E_{N_\pi}\{\psi_A(\theta(1 - s), K \cap \pi)^{N_\pi}\} \\ &= \exp[\theta_2 M(K)(\psi_A(\theta(1 - s), K \cap \pi) - 1)]. \end{aligned}$$

□

The generating function $G(s, r)$ of the random number of points $N_P(r)$ in the sphere with radius r is given by

$$G(s, r) = \exp[-4\pi r \theta_2(1 - \psi(\theta\pi(1 - s), r))]$$

and

$$1 - T(r) = Q(r) = \exp[-4\pi r \theta_2(1 - \psi(\theta\pi, r))]$$

with (see equation (7.4))

$$\psi(\lambda, r) = \frac{\exp(-\lambda r^2) \int_0^{r\sqrt{\lambda}} \exp(y^2) dy}{r\sqrt{\lambda}}.$$

3.3. Poisson points on Poisson lines in \mathbb{R}^3 . This point process is obtained in two steps:

- (1) We start from isotropic Poisson lines in \mathbb{R}^3 , with intensity θ_1 .
- (2) On each Poisson line, a 1D Poisson point process with intensity θ is generated.

Proposition 7. *The generating function $G_K(s)$ of the random number of points $N_D(K)$ contained in a convex set K is given by*

$$(3.9) \quad G_K(s) = \exp\left[-\frac{\pi}{4}\theta_1 S(K)(1 - \varphi_L(\theta(1 - s), K))\right]$$

so that

$$(3.10) \quad 1 - T(K) = Q(K) = \exp\left[-\frac{\pi}{4}\theta_1 S(K)(1 - \varphi_L(\theta, K))\right],$$

where $S(K)$ is the surface area of K , and $\varphi_L(\lambda, K)$ is the Laplace transform of a random chord $L(K)$ in K .

The Choquet capacity of the corresponding Boolean model for convex sets K and A' is obtained by replacing K by $(A' \oplus \check{K})$ in equation (3.10).

P r o o f. The random number of lines $N_D(K)$ hit by K is a Poisson variable with parameter $\frac{1}{4}\pi\theta_1 S(K)$. Each line cuts K along a random chord with length $L(K)$, containing a Poisson number of points with parameter $\theta L(K)$ and with generating function

$$\Gamma(s, L(K)) = \exp(\theta L(K)(s - 1)).$$

After deconditioning with respect to $L(K)$, with Laplace transform $\varphi_L(\lambda, K)$, we obtain the generating function $\Gamma(s, K) = E_L\{\Gamma(s, L(K))\} = \varphi_L(\theta(1 - s), K)$. Then we consider the sum of N_D realizations of the random variable $L(K)$ to obtain equation (3.9) by expectation with respect to N_D :

$$G_K(s) = E_{N_D}\{\varphi_L(\theta(1 - s), K)^{N_D}\} = \exp\left[-\frac{\pi}{4}\theta_1 S(K)(1 - \varphi_L(\theta(1 - s), K))\right].$$

□

The generating function $G(s, r)$ of the random number of points $N_P(r)$ in the sphere with radius r is expressed by

$$\log(G(s, r)) = -\pi^2\theta_1 r^2 \left(1 - \frac{2}{(2r\theta(1 - s))^2} [1 - (1 + 2r\theta(1 - s)) \exp(-2r\theta(1 - s))]\right)$$

and

$$1 - T(r) = Q(r) = \exp\left[-\pi^2\theta_1 r^2 \left(1 - \frac{2}{(2r\theta)^2} [1 - (1 + 2r\theta) \exp(-2r\theta)]\right)\right].$$

4. THREE-STEPS POISSON POINTS IN \mathbb{R}^3

A new point process is obtained by a three steps iteration: Poisson points on 2D Poisson lines contained in Poisson planes.

- (1) We start from Poisson planes in \mathbb{R}^3 (isotropic case), with intensity θ_2 .
- (2) On each Poisson plane, a 2D Poisson lines process with intensity θ_1 is generated.
- (3) On each line, a 1D Poisson point process with intensity θ is given.

Proposition 8. *Consider a convex compact set K , with random planar sections $K \cap \pi$. The generating function $G_K(s)$ of the random number of points $N_D(K)$ contained in the convex set K is given by*

$$(4.1) \quad \log(G_K(s)) = -\theta_2 M(K) (E_\pi \{ \exp[\theta_1 \mathcal{L}(K \cap \pi) (\varphi_L(\theta(1-s), K \cap \pi) - 1)] \} - 1),$$

where E_π is the mathematical expectation over random sections. We get

$$(4.2) \quad \begin{aligned} \log(1 - T(K)) &= \log(Q(K)) \\ &= -\theta_2 M(K) (E_\pi \{ \exp[\theta_1 \mathcal{L}(K \cap \pi) (\varphi_L(\theta, K \cap \pi) - 1)] \} - 1) \end{aligned}$$

with perimeter $\mathcal{L}(K \cap \pi)$ of sections of K , with Laplace transform $\psi_{\mathcal{L}}(\lambda, K \cap \pi)$, random chord of each planar section $L(K \cap \pi)$, with Laplace transform $\varphi_L(\lambda, K \cap \pi)$.

The Choquet capacity of the corresponding Boolean model for convex sets K and A' is obtained by replacing K by $(A' \oplus \check{K})$ in equation (4.2).

P r o o f. The random number of planes $N_\pi(K)$ hit by K is a Poisson variable with parameter $\theta_2 M(K)$. Each plane π cuts K along to a convex random set with random perimeter $\mathcal{L}(K \cap \pi)$ hitting a Poisson number of lines, with parameter $\theta_1 \mathcal{L}(K \cap \pi)$. Each line cuts $K \cap \pi$ along a random chord $L(K \cap \pi)$ containing a Poisson number of points with parameter $\theta L(K)$ and generating function

$$\Gamma(s, L(K \cap \pi)) = \exp(-\theta L(K \cap \pi)(1 - s)).$$

For a given section $K \cap \pi$, the generating function of the number of points on a line is obtained by deconditioning over $L(K \cap \pi)$, so that

$$\Gamma(s, K \cap \pi) = \varphi_L(\theta(1 - s), K \cap \pi).$$

The generating function of the random number of points on $K \cap \pi$ is given by the expectation of $\Gamma(s, K \cap \pi)^N$, N being the Poisson variable with parameter $\theta_1 \mathcal{L}(K \cap \pi)$, and therefore,

$$E\{\Gamma(s, K \cap \pi)^N\} = \exp[\theta_1 \mathcal{L}(K \cap \pi) (\varphi_L(\theta(1 - s), K \cap \pi) - 1)].$$

Deconditioning with respect to the random section $K \cap \pi$ gives

$$\Gamma(s, K) = E_{\pi}\{\exp[\theta_1 \mathcal{L}(K \cap \pi)(\varphi_L(\theta(1-s), K \cap \pi) - 1)]\}.$$

Deconditioning now with respect to the Poisson number of planes $N_{\pi}(K)$, we take the expectation of $\Gamma(s, K)^{N_{\pi}(K)}$ to get equation (4.1). \square

The generating function of the number of points of the process inside a sphere with radius r is given by

$$\log(G(s, r)) = -4\pi\theta_2 r(1 - E_R\{\exp[2\pi\theta_1 R(\varphi_L(\theta(1-s), R) - 1)]\})$$

with

$$\begin{aligned} E_R\{\exp[2\pi\theta_1 R(\varphi_L(\theta(1-s), R) - 1)]\} \\ = \int_0^r \exp[2\pi\theta_1 u(\varphi_L(\theta(1-s), u) - 1)]f(u, r) du, \end{aligned}$$

where

- ▷ $f(u, r)$ is the distribution function of the radius R of random sections of a sphere.
- ▷ $\varphi_L(\lambda, R)$ is the Laplace transform of random chords of the disc with radius R .

The Choquet capacity for a sphere with radius r is given by

$$\begin{aligned} \log(1 - T(r)) &= \log(Q(r)) \\ &= -4\pi\theta_2 r \left(1 - \int_0^r \exp[2\pi\theta_1 u(\varphi_L(\theta, u) - 1)]f(u, r) du\right). \end{aligned}$$

5. USE OF ITERATED BOOLEAN VARIETIES FOR PROBABILISTIC MODELS OF FRACTURE BASED ON THE WEAKEST LINK ASSUMPTION

The standard weakest link model is based on the assumption that fracture in a brittle material is initiated on the most critical defect which controls the full fracture process. For this model, it means that when there is at least one point x in a specimen, where the applied principal stress component $\sigma(x)$ is larger than the local critical stress $\sigma_c(x)$ (i.e. the level of stress for which a fracture is initiated), the specimen is broken. Usually it is assumed that the occurrence or absence of critical defects (generating fracture) of any volume elements generate a set of independent events. After a decomposition of the volume V into links v_i and assuming that there

is a fracture of the volume V when a single link v_i is broken, a classical computation for independent events gives

$$P\{\text{Non fracture}\} = \prod_i P\{\text{Non fracture of } v_i\}.$$

For $v_i \rightarrow 0$, $P\{\text{fracture}\} \simeq \Phi((\sigma(x)) dx$, with Φ increasing with the loading σ and $P\{\text{Non fracture of } dx\} \simeq 1 - \Phi((\sigma(x)) dx$. Therefore with these assumptions,

$$P\{\text{Non fracture of } V\} = \exp\left(-\int_V \Phi(\sigma(x)) dx\right) = \exp(-V\Phi(\sigma_{eq})),$$

where the equivalent stress is defined by

$$\Phi(\sigma_{eq}) = \frac{1}{V} \int_V \Phi((\sigma(x)) dx.$$

This assumption is equivalent to a distribution of point defects in a matrix with $\sigma_c = \infty$, according to a Poisson point process in space (see [6]), with intensity $\Phi(\sigma)$, where $\Phi(\sigma)$ is the average number per unit volume of defects with a critical stress σ_c lower than σ .

For a homogeneous applied stress field $\sigma(x) = \sigma$,

$$P\{\text{Non fracture of } V\} = \exp(-V\Phi(\sigma)).$$

For the Weibull model, the function $\Phi(\sigma)$ is a power law in σ : $\Phi(\sigma) = \theta(\sigma - \sigma_0)^m$ and $P\{\text{Non fracture of } V\}$ follows a 3 parameters Weibull distribution.

The weakest link model corresponds to an ‘‘Infimum’’ Boolean random function with point support primary random functions (PRF), and is immediately extended to any PRF with a support having almost surely compact sections (see [4], [7], [8], [10]).

In what follows the weakest link model is extended to the case of the various point processes introduced in the preceding parts of this paper. It allows for clustering of defects on Poisson varieties. A comparison is made with the standard Poisson-based model and between the various models, when using the same function $\Phi(\sigma)$ for point defects.

5.1. Fracture statistics for Poisson point defects on Poisson lines in \mathbb{R}^2 .

As seen before, a two steps point process can be used to locate random defects:

- (1) Poisson lines in \mathbb{R}^2 (isotropic case), with intensity θ_1 .
- (2) On each Poisson plane, a 1D Poisson point process of point defects acting in fracture, with intensity θ replaced by $\Phi(\sigma)$ in equation (3.6).

We get

$$(5.1) \quad P\{\sigma_R \geq \sigma\}_L = \exp(-\theta_1 \mathcal{L}(K)(1 - \varphi_L(\Phi(\sigma), K))).$$

When K is the disc with radius r ,

$$(5.2) \quad P\{\sigma_R \geq \sigma\}_L = Q(r, \sigma) = \exp[2\pi r \theta_1 (\varphi_L(\Phi(\sigma), r) - 1)].$$

5.2. Comparison of fracture statistics for Poisson points and for points on lines in \mathbb{R}^2 . In the plane, the average number of Poisson points contained in the disc of radius r is

$$E\{N_P(r)\} = \pi r^2 \theta_2.$$

The average number of Poisson lines hit by the disc is $2\pi r \theta_1$. Therefore, the average number of points of the two-step process on lines is $2\pi r \theta_1 \theta E\{L\}$, $E\{L\}$ being the average chord of the disc. We have $-\pi K'(0) = 2\pi r$ and then $-K'(0) = 2r$, so that $E\{L\} = \pi r^2 / 2r = \pi r / 2$. The average number of points on lines is given by

$$E\{N_P(r)\} = 2\pi r \theta_1 \theta \pi \frac{r}{2} = \pi^2 r^2 \theta_1 \theta.$$

To compare the two fracture statistics, we consider the same average number of defects in the disc, so that we have to use

$$\theta_2 = \pi \theta_1 \theta.$$

We have

$$\begin{aligned} & \log(P\{\sigma_R \geq \sigma\}_P) - \log(P\{\sigma_R \geq \sigma\}_L) \\ &= 2\pi r \theta_1 \left(1 - \varphi_L(\theta, r) - \frac{\pi \theta_1 \theta}{2\pi r \theta_1} \pi r^2\right) \\ &= 2\pi r \theta_1 \left(1 - \varphi_L(\theta, r) - \theta \frac{\pi}{2} r\right). \end{aligned}$$

Using the parameter $\alpha = 2\theta r$, we have to compute

$$2\pi r \theta_1 \left(1 - \frac{\pi}{2} (\text{StruveL}(-1, \alpha) - \text{BesselI}(1, \alpha)) - \frac{\pi}{4} \alpha\right).$$

From numerical calculation, it turns out that this expression remains negative for any α and then

$$(P\{\sigma_R \geq \sigma\}_P) < P\{\sigma_R \geq \sigma\}_L.$$

This result is satisfied for any intensity $\Phi(\sigma)$. In 2D, it is easier to break a specimen with Poisson point defects than with point defects on Poisson lines.

5.3. Fracture statistics for Poisson point defects on Poisson planes in \mathbb{R}^3 .

As earlier, we locate point defects according to a two steps point process:

- (1) Poisson planes in \mathbb{R}^3 (isotropic case), with intensity θ_2 .
- (2) On each Poisson plane, 2D Poisson point process of point defects, with intensity θ replaced by $\Phi(\sigma)$ in equation (3.8).

Considering the Poisson tessellation generated by Poisson planes, this model figures out point defects located on grain boundaries, generating intergranular fracture. We get

$$(5.3) \quad P\{\sigma_R \geq \sigma\}_\pi = \exp[-\theta_2 M(K)(1 - \psi_A(\Phi(\sigma), K \cap \pi))].$$

In the case of a spherical specimen with radius r ,

$$(5.4) \quad P\{\sigma_R \geq \sigma\}_\pi = \exp[-4\pi r \theta_2 (1 - \psi(\pi\Phi(\sigma), r))]$$

with $\psi(\lambda, r)$ given by equation (7.4).

5.4. Fracture statistics for Poisson point defects on Poisson lines in \mathbb{R}^3 .

A model of long fiber network with point defects is obtained from Poisson lines, where we replace θ by $\Phi(\sigma)$ in equation (3.10):

$$(5.5) \quad P\{\sigma_R \geq \sigma\}_D = \exp\left[-\frac{\pi}{4}\theta_1 S(K)(1 - \varphi_L(\Phi(\sigma), K))\right].$$

In the case of a spherical specimen with radius r ,

$$(5.6) \quad P\{\sigma_R \geq \sigma\}_D = \exp\left[-\pi^2\theta_1 r^2\left(1 - \frac{2}{(2r\Phi(\sigma))^2}\right) \times [1 - (1 + 2r\Phi(\sigma))\exp(-2r\Phi(\sigma))]\right].$$

5.5. Comparison of fracture statistics for Poisson points and for points on planes. We consider the fracture of a sphere of radius r containing a random number of points $N_P(r)$ with a given average.

For the standard Poisson point process,

$$E\{N_P(r)\} = \frac{4}{3}\pi r^3 \theta_3.$$

For Poisson points on Poisson planes,

$$E\{N_P(r)\} = \frac{8}{3}\pi^2 r^3 \theta_2 \theta.$$

For a fixed average number of defects in the sphere of radius r , we get

$$\theta_3 = 2\pi\theta_2\theta.$$

Using the same intensity $\Phi(\sigma) = \theta$ for the two processes, we obtain

$$\log(P\{\sigma_R \geq \sigma\}_P) - \log(P\{\sigma_R \geq \sigma\}_\pi) = 4\pi r\theta_2 \left(1 - \psi(\theta\pi, r) - \frac{\theta r^2}{2}\right)$$

and

$$P\{\sigma_R \geq \sigma\}_\pi < P\{\sigma_R \geq \sigma\}_P \quad \text{for } r^2\Phi(\sigma) < 1.8.$$

Given the same statistics of defects $\Phi(\sigma)$, for low applied stresses, or at a small scale, the “intergranular” fracture probability is higher than the standard probability of fracture. For high applied stresses the reverse is true, and the material is less sensitive to “intergranular” fracture. The two probability curves cross for $r^2\Phi(\sigma) \simeq 1.8$.

5.6. Comparison of fracture statistics for Poisson points and for points on lines. We consider again the fracture of a sphere of radius r containing a random number of points $N_P(r)$ with a given average.

For the standard Poisson point process,

$$E\{N_P(r)\} = \frac{4}{3}\pi r^3\theta_3.$$

For Poisson points on Poisson lines,

$$E\{N_P(r)\} = \frac{4}{3}\pi^2 r^3\theta_1\theta.$$

Given the average number of defects in the sphere of radius r , we have

$$\theta_3 = \pi\theta_1\theta.$$

Using the same intensity $\Phi(\sigma) = \theta$ for the two processes, and the auxiliary variable $\alpha = 2r\theta$, we have

$$\begin{aligned} & \log(P\{\sigma_R \geq \sigma\}_D) - \log(P\{\sigma_R \geq \sigma\}_P) \\ &= \pi^2\theta_1 r^2 \left(\frac{2}{\alpha^2} (1 - (1 + \alpha)\exp(-\alpha)) - 1 + \frac{2}{3}\alpha \right) \end{aligned}$$

and

$$P\{\sigma_R \geq \sigma\}_D < P\{\sigma_R \geq \sigma\}_P.$$

Therefore, given the same statistics of defects $\Phi(\sigma)$, the “fiber” fracture probability is higher than the standard probability of fracture. The material is more sensitive to point defects on fibers.

5.7. Comparison of fracture statistics for Poisson points on planes and for points on lines. For a given average number of defects in the sphere of radius r , we have

$$\theta_2\theta_\pi = \frac{1}{2}\theta_1\theta_D.$$

Taking $2r\theta_D = \pi r^2\theta_\pi = \alpha$, we get $\pi^2\theta_1r^2 = 4\pi r\theta_2$. Using the same intensity $\Phi(\sigma) = \theta = \theta_\pi = \theta_D$ for the two processes, we get

$$\begin{aligned} & \log(P\{\sigma_R \geq \sigma\}_\pi) - \log(P\{\sigma_R \geq \sigma\}_D) \\ &= \pi^2\theta_1r^2 \left(\psi(\theta\pi, r) - \frac{2}{\alpha^2}(1 - (1 + \alpha)\exp(-\alpha)) \right) > 0, \end{aligned}$$

therefore $P\{\sigma_R \geq \sigma\}_\pi > P\{\sigma_R \geq \sigma\}_D$ for any distribution $\Phi(\sigma)$ of defects and it is easier to break a specimen with defects on fibers than with defects on planes.

5.8. Fracture statistics for defects obtained in the three steps iteration.

We consider now a model of long fibers in random planes, with point defects located on the fibers, where θ is replaced by $\Phi(\sigma)$ in equation (4.2). We have

$$\log(P\{\sigma_R \geq \sigma\}_{3 \text{ iterations}}) = \theta_2M(K)(E_\pi\{\exp[\theta_1\mathcal{L}(K \cap \pi)(\varphi_L(\Phi(\sigma), K \cap \pi) - 1)]\} - 1).$$

For fracture statistics of the sphere with radius r ,

$$\log(P\{\sigma_R \geq \sigma\}_{3 \text{ iterations}}) = 4\pi\theta_2r \left(\int_0^r \exp[2\pi\theta_1u(\varphi_L(\Phi(\sigma), u) - 1)]f(u, r) du - 1 \right).$$

5.9. Comparison of fracture statistics for Poisson points and for the three steps iteration. We study the fracture statistics of a sphere of radius r containing a random number of points $N_P(r)$ with a given average.

For the standard Poisson point process,

$$E\{N_P(r)\} = \frac{4}{3}\pi r^3\theta_3.$$

For Poisson points on Poisson lines on Poisson planes,

$$E\{N_P(r)\} = \frac{4}{3}\pi r^3(\theta_2\theta_1\theta_2\pi^2).$$

Given an average number of defects in the sphere of radius r , we have

$$\theta_3 = 2\pi^2\theta_2\theta_1\theta.$$

To compare fracture statistics of Poisson points and of the three iterations case, we use the ratio

$$\frac{4}{3} \frac{\theta_3 r^3}{4\theta_2 r} = \frac{4}{3} \frac{2\pi^2\theta_2\theta_1\theta}{4\theta_2} r^2 = \frac{2}{3} \pi^2\theta_1\theta r^2.$$

With auxilliary variables $2\theta r = \alpha$ and $\theta_1 r = \beta$, we have to compare $\frac{1}{3}\pi^2\theta_1\alpha r = \frac{1}{3}\pi^2\alpha\beta$ to

$$1 - \int_0^r \exp[-2\pi\theta_1 u(1 - \varphi_L(\varphi_L(\theta, u)))] f(u, r) dr.$$

Using $u/r = y$ and $du = r dy$, we get

$$\begin{aligned} 1 - \int_0^1 \exp[-2\pi\theta_1 r y(1 - \varphi_L(\theta, r y))] \frac{y}{\sqrt{1-y^2}} dy \\ = 1 - \int_0^1 \exp[-2\pi\beta y(1 - \varphi_L(\theta, r y))] \frac{y}{\sqrt{1-y^2}} dy. \end{aligned}$$

We make a comparison by numerical calculation of the integral over α , for a given β . For $\beta = 0.01, 0.1, 1$, and 10 ,

$$P\{\sigma_R \geq \sigma\}_{3 \text{ iterations}} > P\{\sigma_R \geq \sigma\}_P.$$

5.10. Comparison of fracture statistics for Poisson points on Poisson planes and for the three steps iteration. We fix the average number of points in the sphere with radius r . For Poisson points on Poisson planes

$$E\{N_\pi(r)\} = \frac{8}{3}\pi^2 r^3 \theta_{2\pi} \theta_\pi$$

and for 3 iterations

$$E\{N_P(r)\}_{3 \text{ iterations}} = \frac{4}{3}\pi r^3 (\theta_2 \theta_1 \theta 2\pi^2).$$

To keep the same average values, we fix

$$2\theta_{2\pi}\theta_\pi = 2\pi\theta_2\theta_1\theta.$$

Taking $\theta_\pi = \theta$ to get the same statistics over points, and θ_2 identical for the two models in order to keep the same scale for the Poisson polyhedra, we get $\pi\theta_1 = 1$ and $\theta_1 = 1/\pi$.

With auxiliary variables $2\theta r = \alpha$ and $\theta_1 r = \beta$, we have to compare

$$1 - \psi(\theta\pi, r)$$

and

$$1 - \int_0^1 \exp[-2\pi\beta y(1 - \varphi_L(\theta, ry))] \frac{y}{\sqrt{1-y^2}} dy.$$

For $\beta = 0.01, 0.1, 0.5$, and 0.75 , numerical calculations give

$$P\{\sigma_R \geq \sigma\}_{3 \text{ iterations}} > P\{\sigma_R \geq \sigma\}_\pi.$$

For $\beta = 1$,

$$\begin{aligned} P\{\sigma_R \geq \sigma\}_{3 \text{ iterations}} &< P\{\sigma_R \geq \sigma\}_\pi && \text{when } \alpha < 1.99, \\ P\{\sigma_R \geq \sigma\}_{3 \text{ iterations}} &> P\{\sigma_R \geq \sigma\}_\pi && \text{when } \alpha > 1.99. \end{aligned}$$

For $\beta = 2, 10$,

$$P\{\sigma_R \geq \sigma\}_{3 \text{ iterations}} < P\{\sigma_R \geq \sigma\}_\pi.$$

6. CONCLUSION

The models of random sets and point processes studied in this paper were designed to simulate some specific clustering of points, namely on random lines in \mathbb{R}^2 and \mathbb{R}^3 and on random planes in \mathbb{R}^3 . A possible application is to model point defects in materials with some degree of alignment. We derived general theoretical results, useful to compare geometrical effects on the sensitivity of materials to fracture. Based on the presented theoretical results, applications can be looked for from statistical experimental data.

7. APPENDIX: LAPLACE TRANSFORMS FOR SECTIONS OF DISCS AND OF SPHERES

7.1. Random chords in a disc of radius r . Let L be the random length of a chord obtained by random sections of the disc with radius r (this means chords given by intersections of the disc by lines with a uniform location along its diameter).

Proposition 9. *The cumulative distribution of the random variable L is given by*

$$P\{L < l\} = 1 - \sqrt{1 - \left(\frac{l}{2r}\right)^2}$$

for $l < 2r$.

Proof. For any convex set A with geometrical covariogram $K(h)$, the distribution $P\{L < l\}$ is given by the expression $1 - K'(h)/K'(0)$, where $K'(h)$ is the projection of $A \cap A_h$ in the direction of vector h . For a disc with radius r in \mathbb{R}^2 we get

$$\left(\frac{h}{2}\right)^2 + \left(\frac{K'(h)}{2}\right)^2 = r^2$$

and then

$$(1 - P\{L < l\})^2 = \left(\frac{K'(l)}{K'(0)}\right)^2 = 1 - \left(\frac{l}{2r}\right)^2.$$

□

The Laplace transform of the distribution of random chords L in a disc with radius r is given by

$$\varphi_L(\lambda, r) = \frac{1}{4r^2} \int_0^{2r} \frac{l \exp(-\lambda l)}{\sqrt{1 - (l/2r)^2}} dl.$$

Using $y = l/2r$ so that $dl = 2r dy$, $\varphi_L(\lambda, r)$ can be derived using the formal computation software Mathematica:

$$\begin{aligned} (7.1) \quad \varphi_L(\lambda, r) &= \frac{1}{4r^2} \int_0^1 \exp(-\lambda 2ry) \frac{2ry 2r}{\sqrt{1-y^2}} dy \\ &= \int_0^1 \exp(-\lambda 2ry) \frac{y dy}{\sqrt{1-y^2}} \\ &= \frac{1}{2} \pi [-\text{BesselI}(1, 2\lambda r) + \text{StruveL}(-1, 2\lambda r)]. \end{aligned}$$

Using the power series for $\exp(-\lambda 2ry) = 1 + \sum_{n=1}^{\infty} (-1)^n (2\lambda r)^n / n!$, we get

$$\int_0^1 \frac{y^n dy}{\sqrt{1-y^2}} = \frac{\sqrt{\pi} \Gamma(\frac{1}{2}(1+n))}{2 \Gamma(1 + \frac{1}{2}n)}$$

and therefore,

$$\begin{aligned} (7.2) \quad \varphi_L(\lambda, r) &= 1 + \frac{\sqrt{\pi}}{2} \sum_{n=1}^{\infty} (-1)^n \frac{(2\lambda r)^n}{n!} \frac{\Gamma(\frac{1}{2}(1+n+1))}{\Gamma(1 + \frac{1}{2}(n+1))} \\ &= 1 + \frac{\sqrt{\pi}}{2} \sum_{n=1}^{\infty} (-1)^n \frac{(2\lambda r)^n}{n!} \frac{\Gamma(\frac{1}{2}(n+2))}{\Gamma(\frac{1}{2}(n+3))}. \end{aligned}$$

7.2. Random radius of sections of a sphere with radius R_3 . The cumulative distribution function of the radius R of a random section of the sphere with radius R_3 is given by

$$P\{R < r\} = 1 - \sqrt{1 - \left(\frac{r}{R_3}\right)^2}.$$

The probability density function is given by

$$(7.3) \quad f(r, R_3) = \frac{r}{R_3^2} \frac{1}{\sqrt{1 - (r/R_3)^2}}.$$

By using $y = r/R_3$ we have $R_3 dy = dr$. The Laplace transform of the distribution of R is given by

$$\begin{aligned} \varphi_R(\lambda, R_3) &= \int_0^{R_3} \frac{r}{R_3^2} \frac{1}{\sqrt{1 - (r/R_3)^2}} \exp(-\lambda r) dr \\ &= \int_0^1 \frac{R_3 y}{R_3^2} \frac{1}{\sqrt{1 - y^2}} R_3 \exp(-\lambda R_3 y) dy \\ &= \int_0^1 \frac{y}{\sqrt{1 - y^2}} \exp(-\lambda R_3 y) dy \\ &= \frac{1}{2} \pi [-\text{BesselI}(1, \lambda R_3) + \text{StruveL}(-1, \lambda R_3)]. \end{aligned}$$

From $\varphi_R(\lambda, R_3)$ we obtain the Laplace transform of the perimeter of sections, $\psi_{\mathcal{L}}(\lambda, B(R_3) \cap \pi)$, by replacing λ by $2\pi\lambda$.

From the distribution of the radius R the Laplace transform of R^2 can be computed:

$$\begin{aligned} E_R\{\exp(-\lambda R^2(R_3))\} &= \psi(\lambda, R_3) \\ &= \int_0^{R_3} \exp(-\lambda u^2) \frac{u}{r^2 \sqrt{1 - (u/R_3)^2}} du. \end{aligned}$$

Using $u/R_3 = y$ and $du = R_3 dy$, we conclude

$$(7.4) \quad \begin{aligned} E_R\{\exp(-\lambda R^2(R_3))\} &= \int_0^1 \exp(-\lambda R_3^2 y^2) \frac{R_3 y R_3 dy}{r^2 \sqrt{1 - y^2}} = \int_0^1 \exp(-\lambda R_3^2 y^2) \frac{y dy}{\sqrt{1 - y^2}} \\ &= \frac{\exp(-\lambda R_3^2) \int_0^{R_3 \sqrt{\lambda}} \exp(y^2) dy}{R_3 \sqrt{\lambda}}. \end{aligned}$$

7.3. Random chords in a sphere with radius R_3 . We start with the geometrical covariogram of the sphere with diameter $a = 2R_3$. For $h < a$,

$$K(h) = V\left(1 - \frac{3h}{2a} + \frac{1}{2}\left(\frac{h}{a}\right)^3\right),$$

$$K'(h) = V\left(-\frac{3}{2}\frac{1}{a} + \frac{3h^2}{2a^3}\right).$$

The cumulative distribution function is obtained by

$$1 - F(l) = \frac{K'(l)}{K'(0)} = 1 - \frac{l^2}{a^2} \quad \text{for } l < a$$

and

$$F(l) = \frac{l^2}{a^2} \quad \text{for } l < a$$

with density

$$f(l) = \frac{2l}{a^2} \quad \text{for } l < a.$$

For a sphere with radius R_3

$$f(l) = \frac{l}{2R_3^2} \quad \text{for } l < 2R_3.$$

The Laplace transform of $f(l)$ is obtained from

$$\varphi_{SL}(\lambda, R_3) = \frac{1}{2R_3^2} \int_0^{2R_3} l \exp(-\lambda l) dl.$$

Using $y = l/2R_3$ with $dy = dl/2R_3$ yields

$$\begin{aligned} \varphi_{SL}(\lambda, R_3) &= \frac{1}{2R_3^2} \int_0^{2R_3} \exp(-\lambda l) 2R_3 y (2R_3) dy \\ &= 2 \int_0^1 \exp(-\lambda 2R_3 y) y dy. \end{aligned}$$

Since

$$\int_0^1 y \exp(-\alpha y) dy = \frac{1 - (1 + \alpha) \exp(-\alpha)}{\alpha^2},$$

we get

$$\varphi_L(\lambda, R_3) = \frac{2}{(2R_3\lambda)^2} [1 - (1 + 2R_3\lambda) \exp(-2R_3\lambda)].$$

Using the power series expansion of $\psi(\lambda, r)$, $\exp(-\lambda r^2 y^2) = 1 + \sum_1^{\infty} (-1)^n (\lambda r^2 y^2)^n / n!$.

We get

$$\int_0^1 \frac{y^{2n+1} dy}{\sqrt{1-y^2}} = \frac{\sqrt{\pi}}{2} \frac{\Gamma(\frac{1}{2}(2n+2))}{\Gamma(1+\frac{1}{2}(2n+1))} = \frac{\sqrt{\pi}}{2} \frac{n!}{\Gamma(n+1+\frac{1}{2})}$$

and

$$\psi(\lambda, r) = \int_0^1 \exp(-\lambda r^2 y^2) \frac{y dy}{\sqrt{1-y^2}} = 1 + \frac{\sqrt{\pi}}{2} \sum_1^{\infty} (-1)^n \frac{(\lambda r^2)^n}{\Gamma(n+1+\frac{1}{2})}.$$

References

- [1] *Ch. Delisée, D. Jeulin, F. Michaud*: Caractérisation morphologique et porosité en 3D de matériaux fibreux cellulósiques. C.R. Académie des Sciences de Paris, t. 329, Série II b (2001), 179–185. (In French.)
- [2] *J. Dirrenberger, S. Forest, D. Jeulin*: Towards gigantic RVE sizes for 3D stochastic fibrous networks. Int. J. Solids Struct. 51 (2014), 359–376.
- [3] *M. Faessel, D. Jeulin*: 3D multiscale vectorial simulations of random models. Proceedings of ICS13 (2011), 19–22.
- [4] *D. Jeulin*: Modèles Morphologiques de Structures Aléatoires et de Changement d’Echelle. Thèse de Doctorat d’Etat ès Sciences Physiques, Université de Caen (1991).
- [5] *D. Jeulin*: Modèles de Fonctions Aléatoires multivariables. Sci. Terre 30 (1991), 225–256. (In French.)
- [6] *D. Jeulin*: Random structure models for composite media and fracture statistics. Advances in Mathematical Modelling of Composite Materials (1994), 239–289.
- [7] *D. Jeulin*: Random structure models for homogenization and fracture statistics. Mechanics of Random and Multiscale Microstructures (D. Jeulin, M. Ostoja-Starzewski, eds.). CISM Courses Lect. 430, Springer, Wien, 2001, pp. 33–91.
- [8] *D. Jeulin*: Morphology and effective properties of multi-scale random sets. A review, C. R. Mécanique 340 (2012), 219–229.
- [9] *D. Jeulin*: Boolean random functions. Stochastic Geometry, Spatial Statistics and Random Fields. Models and Algorithms (V. Schmidt, ed.). Lecture Notes in Mathematics 2120, Springer, Cham, 2015, pp. 143–169.
- [10] *D. Jeulin*: Power laws variance scaling of Boolean random varieties. Methodol. Comput. Appl. Probab., 2015, pp. 1–15, DOI: 10.1007/s11009-015-9464-5.
- [11] *R. Maier, V. Schmidt*: Stationary iterated tessellations. Adv. Appl. Probab. 35 (2003), 337–353.
- [12] *G. Matheron*: Random Sets and Integral Geometry. Wiley Series in Probability and Mathematical Statistics, John Wiley & Sons, New York, 1975.
- [13] *W. Nagel, V. Weiss*: Limits of sequences of stationary planar tessellations. Adv. Appl. Probab. 35 (2003), 123–138.
- [14] *K. Schladitz, S. Peters, D. Reinel-Bitzer, A. Wiegmann, J. Ohser*: Design of acoustic trim based on geometric modeling and flow simulation for non-woven. Computational Materials Science 38 (2006), 56–66.

Author’s address: Dominique Jeulin, MINES ParisTech, PSL Research University, CMM-Centre de Morphologie Mathématique 35, rue Saint Honoré, F-77305 Fontainebleau, France, e-mail: dominique.jeulin@mines-paristech.fr.